


## Pairing of electromagnetic bosons under spin-orbit coupling

S. V. Andreev \*

Abrikosov Center for Theoretical Physics, Moscow Institute of Physics and Technology, Dolgoprudny 141700, Russia;  
Smart Software Solutions, Saint-Petersburg 191014, Russia;

and National Research Center Kurchatov Institute B.P. Konstantinov, Petersburg Nuclear Physics Institute, Gatchina 188300, Russia



(Received 17 November 2021; revised 14 October 2022; accepted 18 October 2022; published 31 October 2022)

We discuss pairing of excitons and polaritons under effective spin-orbit coupling in two-dimensional semiconductors. The spin-orbit coupling is shown to induce dynamical broadening of a two-body bound state. Application of a transverse magnetic field yields the rich Feshbach resonance phenomenology. We predict quantum bosonic halos with a synthetic angular momentum  $L_z = \pm 2\hbar$ . The  $d$ -wave-like dressing of the nominally  $s$ -wave bound state is induced by spin-orbital coupling to the continuum in the open channel. As a possible manifestation of the phenomenon in the equilibrium phase diagram we predict *biexcitonic Mott supercurrent*: Dissociation of a biexciton Bose-Einstein condensate into a superfluid current of excitons upon increasing the density.

DOI: [10.1103/PhysRevB.106.155157](https://doi.org/10.1103/PhysRevB.106.155157)

### I. INTRODUCTION

Strongly correlated pairs of photons have been of paramount interest for fundamental and applied quantum science [1–4]. In the semiconductor technology pairing of electromagnetic waves is enabled by formation of a biexcitonic molecule. Quantum entanglement of photon pairs has been experimentally demonstrated with biexcitons in semiconductor quantum dots [5,6] and nanocrystals [7]. Further progress toward greater functionalities would require controllable pairing in macroscopic ensembles of light-matter bosons [2–4,8]. Observation of biexcitons in several prominent classes of two-dimensional (2D) semiconductors [8–15] has spurred an intense theoretical research in the field over the past years (see [16] and references therein).

Bosonic modes in planar semiconductors have fine structure due the long-range exchange interaction of the constituent fermions [17–23] and TE-TM splitting of the associated electromagnetic field [24–26]. Both contributions can be regarded as interaction of the boson spin with a momentum-dependent effective magnetic field. The influence of such effective spin-orbit (SO) coupling on the boson pairing is an interesting question, which has been addressed only scarcely in our recent studies [27].

In this paper we present a theoretical approach to the problem based on the method of second quantization. We construct a generic pairing Hamiltonian amenable to simple mean-field models for macroscopic ensembles and multichannel scattering formalism for two particles in vacuum. The SO interaction couples bound states to continua in the channels with different spin configurations. Application of a static magnetic field along  $z$  (the Faraday geometry) yields a rich phenomenology akin to the Feshbach resonance in ultracold

atomic gases [28]. We obtain analytical estimates of the positions of resonances for 2D excitons and polaritons. Close to the resonance we predict macroscopic bosonic molecules (the so-called halo states [29]) possessing an angular momentum  $L_z = \pm 2\hbar$ . The nominally  $s$ -wave bound state acquires a  $d$ -wave-like halo due to the SO coupling with the continuum. Straightforward extension of our formalism indicates that one may expect existence of analogous mechanisms for fermions. As a possible manifestation of the phenomenon in the equilibrium phase diagram we predict *biexcitonic Mott supercurrent*: Dissociation of a biexciton Bose-Einstein condensate into a superfluid current of excitons upon increasing the density. Fundamental properties of the emergent quantum number and the associated many-body states, as well as their possible use in quantum technologies, remain to be explored.

### II. THEORETICAL MODEL

The electromagnetic boson fields in a 2D semiconductor are guided (surface) exciton-polaritons propagating in the structure plane. At low momenta inside the light cone there is either rapid radiative decay [30] or hybridization with a cavity mode [31]. The latter results in a strong reduction of the polariton effective mass. We shall neglect leakage of the polariton modes from the cavity. For excitons, we assume that their momenta are outside of the light cone.

The optical selection rules lock the photon spin to the spin orientation of an electron and a hole constituting the exciton. In considering the exciton-exciton interactions this will allow us to conveniently avoid cumbersome and system-specific analysis accounting for all possible spin configurations of four fermions [32–34]. Our approach extends to a broad variety of 2D semiconductor structures where the concomitant symmetries (e.g., valleys in the absence of an inversion center [35], short-range electron-hole exchange [17], etc.) or cavity-induced detunings isolate the radiative doublet from

\*Serguey.Andreev@gmail.com

other exciton states (e.g., dark excitons [36]). A quantitative criterion will be formulated below. Virtual transmutations of the electromagnetic bosons into satellite states then may be regarded as a background renormalization of the relevant quantities [37]. We shall bear in mind atomically thin layers of transition-metal dichalcogenides (TMD's), such as MoS<sub>2</sub>, as primary experimental test beds.

### A. Single-particle Hamiltonians

The single-particle Hamiltonian may be written as

$$\hat{H}_{\alpha,i} = \left[ K_{\alpha}(\hat{\mathbf{p}}_i) + \frac{\delta_{\alpha}(B)}{2} \right] \hat{1}_i - \hbar \boldsymbol{\omega}_{\alpha}(\hat{\mathbf{p}}_i) \cdot \hat{\mathbf{s}}_i \quad (1)$$

with the Larmor frequency

$$\boldsymbol{\omega}_{\alpha}(\hat{\mathbf{p}}) = \boldsymbol{\Omega}_{\alpha}(\hat{\mathbf{p}}) + \frac{\mu_B}{\hbar} \mathbf{g}_{\alpha} B \mathbf{n}_z \quad (2)$$

being due to the ordinary magnetic field  $B$  and the in-plane effective SO field

$$\boldsymbol{\Omega}_{\alpha}(\hat{\mathbf{p}}) = \Omega_{x,\alpha}(\hat{\mathbf{p}}) \mathbf{n}_x + \Omega_{y,\alpha}(\hat{\mathbf{p}}) \mathbf{n}_y \quad (3)$$

constructed on the basis of the momentum operator  $\hat{\mathbf{p}} = (\hat{p}_x, \hat{p}_y)$ . The index  $i$  in (1) is introduced to label the particles. The label  $\alpha$  distinguishes between the exciton ( $\alpha = X$ ) and lower-polariton ( $\alpha = L$ ) models. For polaritons, we assume large vacuum Rabi splitting  $\hbar \Omega_R(B)$  as compared to the detuning  $\delta_{\pm} = \delta_0 - \delta_X(B) \pm \mu_B \mathbf{g}_X B$  between the microcavity and the exciton modes. Here  $\delta_0$  is the nominal ( $B = 0$ ) detuning and  $\delta_X(B)$  is the exciton diamagnetic shift [38,39]. At the bottom of the dispersion, where Eqs. (7) hold, one has  $\delta_L(B) = \delta_X(B)/2 + \delta_0 - \hbar \Omega_R(B)$  and  $\mathbf{g}_L = X_0^2 \mathbf{g}_X$  with  $X_0^2 = 1/2[1 + (1 + \hbar^2 \Omega_R^2 / \delta_{\pm}^2)^{-1/2}] \approx 1/2$  being the Hopfield coefficient  $X_p^2$  evaluated at  $\mathbf{p} = 0$  [38]. All polariton parameters vary along the dispersion curve and approach their bare excitonic values at high momenta.

By virtue of the optical selection rules, the boson spin  $\hat{\mathbf{s}}$  may be identified with the spin-1 operator of a transverse electromagnetic field [40], i.e.,

$$\hat{\mathbf{s}} = \hat{\sigma}_x \mathbf{n}_x + \hat{\sigma}_y \mathbf{n}_y + \hat{\sigma}_z \mathbf{n}_z. \quad (4)$$

Here  $\hat{\sigma}_x$ ,  $\hat{\sigma}_y$ , and  $\hat{\sigma}_z$  are Pauli matrices, and  $\mathbf{n}_x$ ,  $\mathbf{n}_y$ ,  $\mathbf{n}_z$  form an orthonormal basis. We shall adopt the notation  $|\uparrow\rangle$  and  $|\downarrow\rangle$  for the basis states characterized by  $s_z = +1$  and  $-1$ , respectively [41]. The three components of an expectation value  $\langle \hat{\mathbf{s}} \rangle$  are the Stokes parameters encoding the photon polarization.

The decomposition of the total magnetic field  $\boldsymbol{\omega}_{\alpha}$  into its in-plane and transverse components adopted in Eq. (2) may be argued as follows. Under the time reversal one has  $\hat{s}_z \rightarrow -\hat{s}_z$ , whereas  $\hat{s}_{x,y} \rightarrow \hat{s}_{x,y}$  [42]. Since, on the other hand,  $\mathbf{B} \rightarrow -\mathbf{B}$ , it follows that the boson spin  $\hat{\mathbf{s}}$  may couple only to the transverse component of  $\mathbf{B}$ . In the electron-hole picture this constraint corresponds to the mere fact that the 2D band orbital momentum does not possess an in-plane component [43–45]. In contrast, the in-plane SO field (3) satisfies

$$\boldsymbol{\Omega}_{\alpha}(\hat{\mathbf{p}}) = \boldsymbol{\Omega}_{\alpha}(-\hat{\mathbf{p}}), \quad (5)$$

which makes possible its coupling to the in-plane components of  $\hat{\mathbf{s}}$ . Explicitly, we shall assume

$$K_X(\mathbf{p}) = \frac{\hbar^2 p^2}{2m_X} + \frac{\hbar v p}{2}, \quad (6a)$$

$$\boldsymbol{\Omega}_X(\mathbf{p}) = -\frac{v p}{2} (\mathbf{n}_x \cos 2\theta + \mathbf{n}_y \sin 2\theta) \quad (6b)$$

for excitons [18–22,27] and

$$K_L(\mathbf{p}) = \frac{\hbar^2 p^2}{2m_*}, \quad (7a)$$

$$\boldsymbol{\Omega}_L(\mathbf{p}) = -\frac{\hbar p^2}{2m_{LT}} (\mathbf{n}_x \cos 2\theta + \mathbf{n}_y \sin 2\theta) \quad (7b)$$

for polaritons [24–27], where  $m_*^{-1} = m_L^{-1} + m_{LT}^{-1}$  with  $m_L$  and  $m_{LT}$  being the lower polariton mass and the parameter characterizing the longitudinal-transverse splitting of the polariton dispersion, respectively. The momentum-dependent shifts of the kinetic energies  $K_{\alpha}(\mathbf{p})$  ensure monotonous behavior of the dressed-particle dispersions obtained by diagonalization of the Hamiltonians (1).

The picture of an electromagnetic boson as a well-defined quasiparticle implicitly assumed in the above models requires that its kinetic energy be larger than the radiative width. Neglecting the exchange-induced corrections to  $K_{\alpha}(\mathbf{p})$ , the corresponding condition may be written as

$$k \gg \sqrt{m_{\alpha} / \hbar \tau_{\alpha}} \quad (8)$$

with  $\tau_{\alpha}$  being the boson radiative lifetime. This lower bound on the in-plane momentum of the quasiparticle defines the accuracy of the low-energy approximation employed below. The exciton radiative lifetime  $\tau_X$  may be increased by placing the semiconductor onto a substrate [46] or into an off-resonant microcavity [47]. One may also work with dipolar excitons formed of spatially separated electrons and holes (see [27] and references therein).

### B. Biexciton and bipolariton in the absence of SO coupling

Binding of light-matter bosons occurs via their excitonic component due to exchange of the identical fermions. A close analog of the biexciton is the positronium molecule Ps<sub>2</sub> [48]. In the spirit of covalent bonding in the molecular hydrogen H<sub>2</sub>, the singlet electrons produce Coulomb attraction for holes and vice versa. Opposite orientations of the fermionic spins imply the singlet configuration for the associated photons. Only even spin and orbital boson wave functions are allowed [49,50]. The orbital wave function  $\varphi_n(\mathbf{r})$  can be obtained as a solution of the Schrödinger equation for the relative motion

$$[K_{\text{rel}}^{(X)}(\hat{\mathbf{k}}) + V_{\uparrow\downarrow}^{(X)}(r)] \varphi_n(\mathbf{r}) = \varepsilon_n \varphi_n(\mathbf{r}), \quad (9)$$

where  $V_{\uparrow\downarrow}^{(X)}(r)$  is an axially symmetric potential describing interaction of two composite bosons [51] and the index  $n$  stands for a full set of possible quantum numbers. The kinetic energy of relative motion  $K_{\text{rel}}^{(X)}(\hat{\mathbf{k}})$  is defined in a standard way via the rearrangement  $K_X(\hat{\mathbf{p}}_1) + K_X(\hat{\mathbf{p}}_2) = K_{\text{rel}}^{(X)}(\hat{\mathbf{k}}) + K_{\text{cm}}^{(X)}(\hat{\mathbf{K}})$  which always holds at least in the center-of-mass (c.m.) reference frame.

In practice, excited states of a biexciton have never been observed. We are also unaware of any theoretical claim of

such states. In fact, studies of the analogous dipositronium problem suggest that such states may actually not exist due to a very diffuse structure of a four-particle complex consisting of electrons and holes with equal masses [52]. We shall therefore assume that the set of bound states labeled by  $n$  in Eq. (16) consists of a single  $s$ -wave (ground) state. This assumption, while not implying any loss of generality, will also highlight the emergent nature of the state derived in this work. We shall use the notations  $\varphi_{1s}(r) \equiv \varphi(r)$  and  $\varepsilon_{1s} \equiv \varepsilon$ , and take the Gaussian *Ansatz*

$$\varphi(r) = (a\sqrt{\pi})^{-1} e^{-r^2/2a^2} \quad (10)$$

for our analytical estimates. Here  $a \equiv \hbar/\sqrt{m_X|\varepsilon|}$  is on the order of the microscopic biexciton radius (few nanometers in TMD's).

Increasing the static transverse dipole moment of a dipolar exciton allows one to tune the biexciton energy  $\varepsilon$  toward zero and even positive values. The latter correspond to the biexciton being transformed into an  $s$ -wave scattering resonance [53,54]. We shall call it *natural* resonance in order to make distinction with the *synthetic* SO-induced scattering resonances predicted in this work. An interplay between the two has to some extent been addressed in our prior work [27]. The object of this study is true bound exciton pairs with  $\varepsilon < 0$  and  $a$  much less than any other relevant length scale. The main control parameter, absent in [27], is the transverse magnetic field.

In a microcavity, the bend of the lower-polariton dispersion in the vicinity of the light cone may produce autodissociation of the biexciton into the polariton continuum [55]. Such quasistationary biexciton has been referred to as ‘‘bipolariton’’ [51]. The autodissociation occurs when the biexciton level crosses the lower-polariton continuum with the singlet spin configuration. The corresponding condition reads as  $\varepsilon + \delta_X(B) > \delta_L(B)$ . The resonant approximation (26) employed below requires that

$$\varepsilon + \delta_X(B) < \delta_L(B) \quad (11)$$

and, therefore, excludes such uncontrollable broadening of the biexciton level.

### C. Pairing Hamiltonian

Consider a system of two particles. There are four basis states  $|\uparrow\uparrow\rangle, |\uparrow\downarrow\rangle, |\downarrow\uparrow\rangle, |\downarrow\downarrow\rangle$  whose linear combinations realize the states  $S_z = +2, 0, -2$  of the total spin  $S_z = s_{z,1} + s_{z,2}$ . We notice that since  $\mathbf{\Omega}_\alpha(\hat{\mathbf{p}}_i)$  lies in the structure plane, the sum  $\mathbf{\Omega}_\alpha(\hat{\mathbf{p}}_1) \cdot \hat{\mathbf{s}}_1 + \mathbf{\Omega}_\alpha(\hat{\mathbf{p}}_2) \cdot \hat{\mathbf{s}}_2$  does not commute with  $S_z^2$ . Hence, the SO coupling may change the spin state of a pair by flipping the spin of either of the two particles. This property in combination with the symmetry relation (5) are the key ingredients for the phenomenology presented in this work.

To proceed, let us introduce the (free) pair creation and annihilation operators

$$\begin{aligned} \hat{C}_{\sigma_1\sigma_2,\mathbf{k},\mathbf{K}}^\dagger &= \hat{a}_{\sigma_1\mathbf{k}+\mathbf{K}/2}^\dagger \hat{a}_{\sigma_2,-\mathbf{k}+\mathbf{K}/2}^\dagger, \\ \hat{C}_{\sigma_1\sigma_2,\mathbf{k},\mathbf{K}} &= \hat{a}_{\sigma_2,-\mathbf{k}+\mathbf{K}/2} \hat{a}_{\sigma_1\mathbf{k}+\mathbf{K}/2}, \end{aligned} \quad (12)$$

where  $\mathbf{k} = (\mathbf{p}_1 - \mathbf{p}_2)/2$  and  $\mathbf{K} = \mathbf{p}_1 + \mathbf{p}_2$  are the relative and center-of-mass (c.m.) momenta, respectively, and  $\sigma = \uparrow, \downarrow$

labels the particle spin. The particle creation (annihilation) operators  $\hat{a}_{\sigma,p}^\dagger$  ( $\hat{a}_{\sigma,p}$ ) obey the usual boson commutation relations. It follows that

$$\hat{C}_{\sigma_1\sigma_2,\mathbf{k},\mathbf{K}} = \hat{C}_{\sigma_2\sigma_1,-\mathbf{k},\mathbf{K}}. \quad (13)$$

Next, we define the molecular operators

$$\hat{C}_{\uparrow\downarrow,n,\mathbf{K}} = \sum_{\mathbf{k}} \phi_n(\mathbf{k}) \hat{C}_{\uparrow\downarrow,\mathbf{k},\mathbf{K}}, \quad (14)$$

where the function  $\phi_n(\mathbf{k})$  is the Fourier image of the molecular wave function of the relative motion

$$\varphi_n(\mathbf{r}) = \frac{1}{\sqrt{S}} \sum_{\mathbf{k}} \phi_n(\mathbf{k}) e^{i\mathbf{k}\mathbf{r}}, \quad (15)$$

defined as an  $\varepsilon < 0$  solution of Eq. (9) and  $S$  is the quantization area. In terms of the free pair and molecular operators the second-quantized *pairing Hamiltonian* can be written as

$$\begin{aligned} \hat{H}_\alpha &= \frac{1}{2} \sum_{\sigma'_1\sigma'_2\sigma_1\sigma_2} \sum_{\mathbf{k}',n',\mathbf{k},n} \\ &\times \sum_{\mathbf{K}',\mathbf{K}} \mathcal{H}_{\sigma'_1\sigma'_2\sigma_1\sigma_2,\alpha}^{\mathbf{k}'(n'),\mathbf{K}',\mathbf{k}(n),\mathbf{K}} \hat{C}_{\sigma'_1\sigma'_2,\mathbf{k}'(n'),\mathbf{K}'}^\dagger \hat{C}_{\sigma_1\sigma_2,\mathbf{k}(n),\mathbf{K}}, \end{aligned} \quad (16)$$

where we have used the obvious notation  $\hat{C}_{\sigma_1\sigma_2,n,\mathbf{K}} \equiv \delta_{\sigma_1\sigma_2} \hat{C}_{\uparrow\downarrow,n,\mathbf{K}}$ . From a mathematical viewpoint, the form (16) is dictated by the principle of asymptotic completeness of the resultant scattering theory [56]. This fundamental principle is expected to hold in our case on timescales shorter than the boson radiative lifetime, i.e., under the assumption (8). The matrix elements

$$\begin{aligned} \mathcal{H}_{\sigma'_1\sigma'_2\sigma_1\sigma_2,\alpha}^{\mathbf{k}'(n'),\mathbf{K}',\mathbf{k}(n),\mathbf{K}} &= \int \psi_{\mathbf{k}'(n'),\mathbf{K}'}^*(\mathbf{r},\mathbf{R}) \langle \sigma'_1\sigma'_2 | \hat{\mathcal{H}}_\alpha | \sigma_1\sigma_2 \rangle \\ &\times \psi_{\mathbf{k}(n),\mathbf{K}}(\mathbf{r},\mathbf{R}) d\mathbf{r} d\mathbf{R} \end{aligned} \quad (17)$$

are taken on the free and bound-state wave functions

$$\psi_{\mathbf{k}\mathbf{K}}(\mathbf{r},\mathbf{R}) = \frac{1}{S} e^{i\mathbf{k}\mathbf{r}+i\mathbf{K}\mathbf{R}}, \quad (18a)$$

$$\psi_{n,\mathbf{K}}(\mathbf{r},\mathbf{R}) = \frac{1}{\sqrt{S}} e^{i\mathbf{K}\mathbf{R}} \varphi_n(\mathbf{r}). \quad (18b)$$

The  $4 \times 4$  matrix Hamiltonian  $\hat{\mathcal{H}}_\alpha$  is given by

$$\hat{\mathcal{H}}_\alpha = \hat{H}_{\alpha,1} \oplus \hat{H}_{\alpha,2} + \hat{V}_\alpha, \quad (19)$$

where ‘‘ $\oplus$ ’’ denotes the Kronecker sum, the  $2 \times 2$  matrices  $\hat{H}_{\alpha,i}$  are given by Eq. (1), and

$$\hat{V}_\alpha = \sum_{\sigma,\sigma'} V_{\sigma\sigma'}^{(\alpha)}(r) |\sigma\sigma'\rangle \langle \sigma\sigma'|. \quad (20)$$

Strictly speaking, the two-body interaction potentials  $V_{\sigma\sigma'}^{(X)}(r)$  are well defined only at interparticle distances  $r$  much larger than the exciton Bohr radius  $a_X$ . This is sufficient, however, for considerations involving the low-energy scattering assumed in our study. Moreover, unless we are interested in long-range physics due to a possible permanent exciton dipole moment [54], the actual shape of the potential curves is not important even at  $r \gg a_X$ . We assume just that the potential  $V_{\uparrow\downarrow}^{(X)}(r)$  possesses a bound state [Eq. (9)], whereas  $V_{\uparrow\uparrow}^{(X)}(r)$  and  $V_{\downarrow\downarrow}^{(X)}(r)$  do not. The Fourier transforms of the lower-polariton

interaction potentials may be obtained in the usual way as  $V_{\sigma\sigma'}^{(L)}(\mathbf{k}' - \mathbf{k}) \equiv X_k^2 X_{k'}^2 V_{\sigma\sigma'}^{(X)}(\mathbf{k}' - \mathbf{k})$ , where  $X_k$  is the Hopfield coefficient.

### III. QUANTUM HALOS

Let us apply our pairing formalism to the single-particle Hamiltonians (1). The external magnetic field splits the triplet of the scattering channels with  $S_z = -2, 0, +2$  by the amount  $2\mu_B g_\alpha B$ . When  $B$  crosses the threshold value  $B_c^{(\alpha)}$  (to be derived below), the lowest-energy scattering states ( $S_z = +2$ ) come into resonance with the  $S_z = 0$  bound state. Assuming  $|B - B_c^{(\alpha)}| \ll B_c^{(\alpha)}$  one may neglect the coupling to the  $S_z = 0, -2$  scattering states (as well as to other possible states such as dark excitons [36]) and reduce the generic Hamiltonian (16) to

$$\begin{aligned} \hat{H}_\alpha = & \sum_{\mathbf{k}} \left[ K_\alpha(\mathbf{k}) + \frac{\delta_\alpha(B)}{2} - \mu_B g_\alpha B \right] \hat{a}_{\uparrow, \mathbf{k}}^\dagger \hat{a}_{\uparrow, \mathbf{k}} \\ & + [\varepsilon + \delta_X(B)] \hat{C}_{\uparrow\downarrow}^\dagger \hat{C}_{\uparrow\downarrow} \\ & + \frac{1}{2S} \sum_{p, p', q} \hat{a}_{\uparrow, p'+q}^\dagger \hat{a}_{\uparrow, p-q}^\dagger V_{\uparrow\uparrow}^{(\alpha)}(\mathbf{q}) \hat{a}_{\uparrow, p} \hat{a}_{\uparrow, p'} \\ & - \sum_{\mathbf{k}} \hbar \mathbf{\Omega}_\alpha^{(s)}(\mathbf{k}) \cdot [s_{\downarrow\uparrow} \phi^*(\mathbf{k}) \hat{C}_{\uparrow\downarrow}^\dagger \hat{a}_{\uparrow, -\mathbf{k}} \hat{a}_{\uparrow, \mathbf{k}} + \text{H.c.}], \end{aligned} \quad (21)$$

where

$$\mathbf{\Omega}_\alpha^{(s)}(\mathbf{k}) = \frac{\mathbf{\Omega}_\alpha(\mathbf{k}) + \mathbf{\Omega}_\alpha(-\mathbf{k})}{2}, \quad (22)$$

$s_{\downarrow\uparrow} \equiv \langle \downarrow | \hat{s} | \uparrow \rangle$  with  $\hat{s}$  defined by Eq. (4),  $\hat{C}_{\uparrow\downarrow}$  is the shortcut for the molecular operator  $\hat{C}_{\uparrow\downarrow, n=1, s, \mathbf{K}=0}$ , and, as usual, we have assumed that all pairs are at  $\mathbf{K} = 0$  in the last term. One may readily recognize the structure of the Fano-Anderson (FA) model of a discrete level in a continuum [57,58]. Mean-field solutions of analogous models have provided much insight into the collective behavior of ultracold atoms with Feshbach resonances [59–61]. The important difference of our system from atomic settings and previously considered dipolar excitons featuring a natural  $s$ -wave resonance [54] is the dynamical (orbital) nature of the coherent coupling between the open ( $S_z = +2$ ) and closed ( $S_z = 0$ ) channels. For two particles in vacuum the Hamiltonian (21) yields the on-shell  $T$  matrix

$$T_{\uparrow\uparrow}^{(\alpha)} = T_{\uparrow\uparrow, \text{bg}}^{(\alpha)} + T_{\uparrow\uparrow, \text{res}}^{(\alpha)}$$

with  $T_{\uparrow\uparrow, \text{bg}}^{(\alpha)}$  being the standard background contribution due to the potential  $V_{\uparrow\uparrow}^{(\alpha)}(\mathbf{k}' - \mathbf{k})$  and

$$T_{\uparrow\uparrow, \text{res}}^{(\alpha)}(\mathbf{k}', \mathbf{k}, E_{\mathbf{k}}^{(\alpha)} + i0) = \frac{2|\tilde{\phi}(\mathbf{k})|^2 |\hbar \mathbf{\Omega}_\alpha^{(s)}(\mathbf{k}) \cdot \mathbf{s}_{\uparrow\downarrow}|^2 e^{2i(\theta' - \theta)}}{E_{\mathbf{k}}^{(\alpha)} - \bar{\Delta}_\alpha - \Pi_\alpha(E_{\mathbf{k}}^{(\alpha)} + i0)}, \quad (23)$$

where

$$\bar{\Delta}_\alpha \equiv \varepsilon + 2\mu_B g_\alpha B + \delta_X(B) - \delta_\alpha(B) \quad (24)$$

is the bare detuning between the channels (note that  $\varepsilon < 0$ ),  $E_{\mathbf{k}}^{(\alpha)} \equiv K_\alpha(\mathbf{k}) + K_\alpha(-\mathbf{k})$  is the kinetic energy of the relative

motion of two bosons,  $\tilde{\phi}(\mathbf{k}) \equiv \sqrt{S} \phi(\mathbf{k}) / 2\pi$  with  $\phi(\mathbf{k})$  defined by Eq. (15), and the pair bubble reads as

$$\Pi_\alpha(E_{\mathbf{k}}^{(\alpha)} + i0) = \int \frac{2|\tilde{\phi}(\mathbf{q})|^2 |\hbar \mathbf{\Omega}_\alpha^{(s)}(\mathbf{q}) \cdot \mathbf{s}_{\uparrow\downarrow}|^2}{E_{\mathbf{k}}^{(\alpha)} - E_{\mathbf{q}}^{(\alpha)} + i0} d\mathbf{q}. \quad (25)$$

The result (23) holds under the conditions

$$|\bar{\Delta}_\alpha| \ll 2\mu_B g_\alpha B \quad (26)$$

and  $|\hbar \mathbf{\Omega}_\alpha^{(s)}(\mathbf{k}) \cdot \mathbf{s}_{\uparrow\downarrow}| \ll \mu_B g_\alpha B$ . The former is the usual resonant approximation, whereas the latter is specific for the problem under consideration. The condition (26) may be seen to imply  $|\varepsilon| \sim \mu_B g_\alpha B$ , so that, under the realistic assumption  $|\varepsilon| \gg |\hbar \mathbf{\Omega}_\alpha^{(s)}(\mathbf{k}) \cdot \mathbf{s}_{\uparrow\downarrow}|$ , the second condition is also fulfilled. The  $d$ -wave-like dependence of  $T_{\uparrow\uparrow, \text{res}}^{(\alpha)}$  on the scattering angle is entirely due to the SO coupling. The bare excitonic molecule has zero orbital momentum.

By using the explicit formulas (6) and assuming  $k \ll m_X v$  we find for the pole of the  $T$  matrix (23) for excitons

$$\begin{aligned} E_X = & \bar{\Delta}_X - \frac{\sqrt{\pi}}{4} E_a^{(X)} - \frac{E_X}{2} \\ & - \frac{\sqrt{\pi}}{2} \frac{E_X^2}{E_a^{(X)}} - \beta_E^{(X)} \ln \left( \frac{E_a^{(X)}}{E_X} \right) - i\pi \beta_E^{(X)}, \end{aligned} \quad (27)$$

where  $\beta_E^{(X)} = E_X^3 / (E_a^{(X)})^2$  and

$$E_a^{(X)} \equiv \hbar v / a. \quad (28)$$

We have used the Fourier transform  $\tilde{\phi}(\mathbf{k}) = \pi^{-1/2} a e^{-k^2 a^2 / 2}$  of the Gaussian Ansatz (10). Solution of Eq. (27) at  $E_X \rightarrow 0$  can be recast in the form

$$E_X(B) = \frac{4}{3} \mu_B g_X (B - B_c^{(X)}), \quad (29)$$

where

$$B_c^{(X)} = (|\varepsilon| + \sqrt{\pi} / 4 E_a^{(X)}) / 2 \mu_B g_X. \quad (30)$$

For polaritons, the massive character of their kinetic energy [Eq. (7a)] allows us to define the scattering amplitude

$$f_{\sigma\sigma'}^{(L)}(\mathbf{k}', \mathbf{k}) = -(2\pi)^2 m_* / 2 \hbar^2 T_{\sigma\sigma'}^{(L)}(\mathbf{k}', \mathbf{k}, E_{\mathbf{k}} + i0).$$

For the resonant contribution we obtain

$$f_{\uparrow\uparrow, \text{res}}^{(L)}(\mathbf{k}', \mathbf{k}) = -\frac{2\pi e^{2i(\theta' - \theta)}}{\frac{\tilde{E}_{\mathbf{k}}^{(L)} - \Delta_L}{\eta^2 (\tilde{E}_{\mathbf{k}}^{(L)})^2 / E_a^{(L)}} + \ln(E_a^{(L)} / E_{\mathbf{k}}^{(L)}) + i\pi}. \quad (31)$$

The amplitude has the genuine  $d$ -wave form. Here  $E_a^{(L)} \equiv \hbar^2 / m_* a^2$  and

$$\eta \equiv \frac{m_*}{\sqrt{2} m_{\text{LT}}}$$

is the dimensionless ratio of the polariton effective mass to the parameter characterizing the strength of the longitudinal-transverse splitting. The renormalized kinetic energy and the detuning read as, respectively,  $\tilde{E}_{\mathbf{k}}^{(L)} = (1 + \eta^2) E_{\mathbf{k}}^{(L)}$  and  $\Delta_L = \bar{\Delta}_L - \eta^2 E_a^{(L)}$ . The pole of the polariton scattering amplitude (31) is given by

$$E_L = (1 + \eta^2)^{-1} \left[ \Delta_L - \beta_E^{(L)} \ln \left( \frac{E_a^{(L)}}{E_L} \right) - i\pi \beta_E^{(L)} \right], \quad (32)$$

where  $\beta_E^{(L)} = \eta^2 E_L^2 / E_a^{(L)}$ . The solution of Eq. (32) at  $E_L \rightarrow 0$  may be written as

$$E_L(B) = (1 + \eta^2)^{-1} \frac{\partial \bar{\Delta}_L}{\partial B} (B - B_c^{(L)}) \quad (33)$$

with

$$B_c^{(L)} = B_0^{(L)} + \eta^2 E_a^{(L)} (\partial \bar{\Delta}_L / \partial B)^{-1} \quad (34)$$

and  $B_0^{(L)}$  being defined by  $\bar{\Delta}_L(B_0^{(L)}) = 0$ .

The solutions (29) and (33) are resonances at  $B > B_c^{(\alpha)}$  and *synthetic* bound states of the two-channel models (21) at  $B < B_c^{(\alpha)}$ . Although the density of states in 2D remains finite at zero energy, the resonances have vanishing widths  $\beta_E^{(\alpha)}$  due to the orbital origin of the effective magnetic fields switching the pair spin configuration. The slopes of the lines  $E_\alpha(B)$  define the relative weights of the bare molecule in the (normalized) wave functions of the synthetic bound states

$$\Psi^{(\alpha)}(\mathbf{r}) = \Upsilon^{(\alpha)}(\mathbf{r}) |\uparrow\uparrow\rangle + w_\alpha \varphi(\mathbf{r}) \frac{1}{\sqrt{2}} (|\uparrow\downarrow\rangle + |\downarrow\uparrow\rangle) \quad (35)$$

via the identity

$$w_\alpha^2 = \left( \frac{\partial \bar{\Delta}_\alpha}{\partial B} \right)^{-1} \left( \frac{\partial E_\alpha}{\partial B} \right).$$

In the vicinity of  $B_c^{(\alpha)}$ , where Eqs. (29) and (33) hold, we obtain  $w_X^2 = \frac{2}{3}$  and  $w_L^2 = (1 + \eta^2)^{-1}$ , respectively. The remaining contributions to the wave functions (35) are due to the quantum halos

$$\Upsilon^{(\alpha)}(\mathbf{r}) = \frac{\sqrt{2} w_\alpha}{\pi} \int \hbar \Omega_\alpha^{(s)}(\mathbf{q}) \cdot s_{\uparrow\downarrow} G_{\uparrow\uparrow}^{(\alpha)}(0) \tilde{\phi}(\mathbf{k}) e^{-i\mathbf{q}\mathbf{r}} d\mathbf{q}, \quad (36)$$

where  $G_{\uparrow\uparrow}^{(\alpha)}(E) = (E - E_q^{(\alpha)})^{-1}$  are the Green functions of the exciton ( $\alpha = X$ ) and polariton ( $\alpha = L$ ) open channels. At  $r \gg a$  we obtain

$$\Upsilon^{(\alpha)}(\mathbf{r}) \propto \frac{a}{r^2} e^{-2i\gamma}, \quad (37)$$

where  $\gamma$  is the polar angle of  $\mathbf{r}$ . In contrast to the strongly localized *s*-wave core, the halos decay algebraically. Most remarkably, the halo carries an angular momentum  $L_z = -2\hbar$  (opposite to the applied magnetic field). We suggest that the emergent quantum number is due to conversion of the core spin fluctuations into the peripheric orbital motion by the SO coupling. In the end of Sec. IV we shall argue that the same mechanism underlies the formation of the polarized superstripe in a resonantly paired superfluid of dipolar excitons [27].

The energy  $E_\alpha(B)$  defined by Eqs. (29) and (33) should not be confused with the dissociation energies of the states described here. The synthetic wave functions (35) themselves represent partially disintegrated states, the halos being quantum superpositions of the continua states in the open channels. Destruction of the halo occurs when the thermal energy  $k_B T$  becomes comparable with the Josephson energies of the coherent SO links between the channels, the latter being on the order of  $E_a^{(X)}$  for excitons and  $\eta E_a^{(L)}$  for polaritons. For excitons in a TMD monolayer, we estimate  $E_a^{(X)}/k_B \sim 150$  K. The same quantity sets the upper bound for the formation time of the composite state (35) and should be compared with the biexciton radiative width (few tens of  $\mu\text{eV}$ ) in order to justify

the picture of well-defined quasiparticles implicitly assumed in our approach. On the other hand, the lower bound (8), as applied to the relative momentum  $k$  of two bosons with  $K = 0$ , defines how far the halo may extend in the real space. For excitons in a MoS<sub>2</sub> monolayer with  $\tau \approx 4$  ps we obtain  $k^{-1} \approx 50$  nm. In comparison, the biexciton radius  $a$  in TMD's amounts to few nanometers [12].

The halo should emit entangled pairs of photons carrying an orbital angular momentum  $-2\hbar$  due to leakage of the low- $k$  excitons into the light cone. Such photons may be detected by using the coincidence circuit supplemented with the forklike interference holograms [62]. We expect  $B_c^{(X)}$  on the order of few tens of teslas which is within reach of the existing experimental facilities [39]. The position of the polariton resonance  $B_c^{(L)}$  as defined by Eq. (34) may be additionally tuned by the Rabi splitting  $\hbar\Omega_R$ .

#### IV. BIEXCITON MOTT SUPERCURRENT

The Hamiltonians (21) provide a basis for the corresponding many-body theories. By virtue of the transient nature of excitons, these are supposed to be nonequilibrium models. Consideration of an equilibrium scenario is, nevertheless, a good starting point to develop a feel for the ensuing phenomena. The central issue for bosons with attractive interaction has been the transition between the particle and molecular Bose-Einstein condensates, the bosonic analog of the BCS-BEC crossover for fermions [63–67]. Excitons have long been considered as promising candidates for realization of this transition [67–70]. In this context, a three-channel Fano-Anderson (FA) model has been suggested for dipolar excitons interacting via a natural *s*-wave resonance [53,54]. The FA model is an advanced version of the old BCS theories and has been put forward during the era of Feshbach-resonant atomic gases [59–61]. The model makes explicit the Goldstone physics associated with the molecular off-diagonal long-range order (ODLRO) and admits an arbitrarily accurate perturbative solution in the limit of a narrow resonance [60,61]. It connects to the variational BCS theory in the opposite limit of a broad resonance.

For a broad resonance the excitonic BCS-BEC transition was also believed to be identical with the so-called biexciton Mott transition [67], associated with the spatial overlap of the molecules at high densities. The *s*-wave FA model had also betrayed the traces of the Mott transition in the reentrant region of the phase diagram corresponding to a true bound state (see the  $\varepsilon < 0$  side of the phase diagram in Fig. 2 in Ref. [53]). This region progressively disappears as one reduces the coupling of the bound state to the (spin-singlet) scattering continuum. On the resonant side ( $\varepsilon > 0$  in the same figure), the prediction of the FA model is opposite to the Mott-type scenario: The quasistationary biexcitons (natural resonances) here are stabilized at increasing density by repulsive interactions.

From this perspective, the Hamiltonians (21) represent qualitatively different variants of the FA model. The *d*-wave-like resonances (27) and (32) being inherently narrow, it is not clear *a priori* whether and how the BCS-BEC transition may be related to the biexciton Mott transition in this case. The most intriguing feature is the *d*-wave SO dressing which produces the quantum halo for a pair of excitons. In the

remainder of the paper we discuss how it may manifest itself in the course of the BCS-BEC transition.

To this end, let us look at the behavior of the pair-breaking excitation spectrum  $\varepsilon_{\uparrow,k}$  on approaching the transition from the BEC side. We focus on the two-channel excitonic ( $\alpha = X$ ) Hamiltonian (21): Excitons, in general, have longer lifetimes as compared to polaritons and may achieve the kinetic equilibrium with respect to the two-body collisions enabling a metastable Bose-Einstein condensed state. We replace the molecular field operator  $\hat{C}_{\uparrow\downarrow}$  by a  $c$  number  $C_{\uparrow\downarrow} \equiv \sqrt{N_B}$  and proceed along the lines of Ref. [27] to obtain

$$\varepsilon_{\uparrow,k} = \sqrt{\zeta_{\uparrow,k}^2 - 4|\hbar\Omega_B^{(s)}(\mathbf{k}) \cdot \mathbf{s}_{\uparrow\downarrow}|^2}, \quad (38)$$

with

$$\zeta_{\uparrow,k} \equiv \frac{\hbar^2 k^2}{2m_X} + \frac{\hbar v k}{2} + g_{XB}|\Psi_B|^2 - \mu_B g_X B - \mu \quad (39)$$

being the (grand canonical) energy of unpaired spin- $\uparrow$  excitons in the mean-field potential produced by the molecules in the absence of the *molecular SO field*

$$\Omega_B^{(s)}(\mathbf{k}) \equiv \sqrt{4\pi n_B a^2} e^{-(ka)^2/2} \Omega_X^{(s)}(\mathbf{k}). \quad (40)$$

In writing Eq. (40) we have used the Gaussian *Ansatz* (10) for  $\phi(\mathbf{k})$ . The occupation number  $N_B$  is related to the molecular order parameter by  $|\Psi_B|^2 = N_B/S \equiv n_B$ . The chemical potential reads as  $\mu = \varepsilon/2 + g_B|\Psi_B|^2/2$ . The phenomenologically introduced coupling constants  $g_B$  and  $g_{XB}$  account for the effective interactions between the molecules and molecules with excitons, respectively. These interactions are expected to be repulsive. Hereinafter, we shall assume  $0 < g_B = g_{XB} \equiv g \ll g_X$ , where  $g_X \equiv g_{\uparrow\uparrow}$  is the effective interaction for the background potential  $V_{\uparrow\uparrow}(\mathbf{q})$ . We define the dimensionless coupling constant  $\tilde{g} \equiv mg/\hbar^2$  and use the value  $\tilde{g} = 1$  in numerical estimates.

In the dilute limit  $n_B a^2 \ll 1$  the molecular SO field is negligible and the gap in the excitation spectrum (38) is located at  $\mathbf{k} = 0$ :

$$\varepsilon_{\uparrow,0} = |\varepsilon|/2 - \mu_B g_X B + n_B(g_{XB} - g_B/2).$$

At the second-order phase transition ray  $\{\mu = \varepsilon/2, \mu_B g_X B < |\varepsilon|/2\}$  separating the biexciton BEC from the vacuum (see Fig. 1) one has  $n_B = 0$ , and the gap is just the energy needed to break a biexciton in free space. As the gas parameter  $n_B a^2$  approaches unity, however, the term (40) becomes important and may overweight the SO shift of the exciton kinetic energy [the second term in Eq. (39)]. In this case the gap shifts to a circle of degenerate minima in the  $\mathbf{k}$  space. Closure of such rotonlike gap marks a second-order (quantum) phase transition into a state discussed below.

A viable candidate for this state is a superposition of counterpropagating plane-wave excitonic condensates  $\psi_{\uparrow,q}$  and  $\psi_{\uparrow,-q}$  with some wave vector  $\mathbf{q} = (q, \theta)$  chosen spontaneously on the circle. The two condensates would be immersed in a residual background of the molecular condensate and share the common phase  $\theta_X$  due to the spontaneously broken  $U_N(1)$  symmetry associated with conservation of the total number of particles  $N = N_X + 2N_B$ . This phase is locked

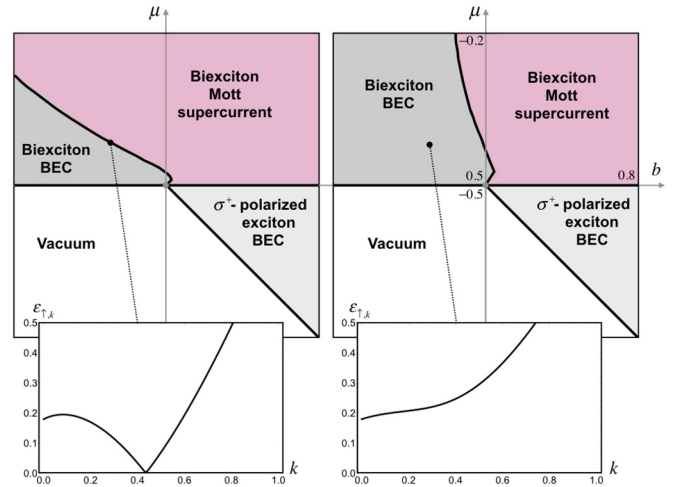


FIG. 1. The zero-temperature phase diagram for the exciton FA model (21) in equilibrium. The biexciton binding energy  $|\varepsilon| \equiv \hbar^2/m_X a^2$  and the characteristic size  $a$  are used as the units of energy and length, respectively. The dimensionless magnetic field reads as  $b \equiv \mu_B g_X B/|\varepsilon|$ . Increasing the chemical potential  $\mu$  (density) at  $b < \frac{1}{2}$  results in dissociation of the biexciton condensate into an exciton supercurrent. The corresponding second-order boundary is defined by closure of the rotonlike gap in the pair-breaking excitation spectrum (shown in the inset). This boundary shifts toward higher magnetic fields and densities as one reduces the strength of the SO coupling  $E_a^{(X)}$  given by Eq. (28) ( $E_a^{(X)} = 0.8$  on the left and  $E_a^{(X)} = 0.5$  on the right). Within our approximation (see the text) the other three boundaries (bold lines) remain unchanged. All four second-order boundaries meet at the quantum critical end point  $(b_c, \mu_c) = (\frac{1}{2}, -\frac{1}{2})$ .

to the molecular background according to the relation

$$\theta_B = 2\theta_X + 2\theta + \pi \quad (41)$$

(modulo  $2\pi$ ), that ensures the maximum energy gain due to the interaction of the exciton spin with the molecular SO field. In order to work out the exact form of the exciton order parameter, we make the substitutions  $\hat{a}_{\uparrow,p}/\sqrt{S} \rightarrow \psi_{\uparrow,\pm q}\delta_{p,\pm q}$  and  $\hat{C}_{\uparrow\downarrow}/\sqrt{S} \rightarrow \sqrt{n_B}e^{i\theta_B}$  in the grand-canonical Hamiltonian  $\hat{H}'_X \equiv \hat{H}_X - \mu\hat{N}$  (supplemented by the  $g_B$  and  $g_{XB}$  terms as outlined above), and diagonalize thus obtained energy density  $h_X$  by the unitary transformation

$$\psi_{\uparrow,q} = \frac{1}{\sqrt{2}}(\psi_+ - \psi_-)e^{i(\theta_B - 2\theta)}, \quad \psi_{\uparrow,-q}^* = \frac{1}{\sqrt{2}}(\psi_+ + \psi_-).$$

We obtain

$$\begin{aligned} h_X = & [\zeta_{\uparrow,q} - 2|\hbar\Omega_B^{(s)}(\mathbf{q}) \cdot \mathbf{s}_{\uparrow\downarrow}|]|\psi_-|^2 \\ & + [\zeta_{\uparrow,q} + 2|\hbar\Omega_B^{(s)}(\mathbf{q}) \cdot \mathbf{s}_{\uparrow\downarrow}|]|\psi_+|^2 \\ & + \frac{g_X}{2}(|\psi_-|^4 + |\psi_+|^4 + 2|\psi_-|^2|\psi_+|^2) \\ & + (\varepsilon - 2\mu)n_B + \frac{g_B}{2}n_B^2. \end{aligned} \quad (42)$$

The energy (42) is minimized by the choice  $\psi_+ \equiv 0$ , which yields  $|\psi_{\uparrow,-q}| = |\psi_{\uparrow,q}|$  and the anticipated Eq. (41) for the phases. The exciton order parameter may finally be recast as

$$\Psi_X(\mathbf{r}) = \sqrt{n_X}e^{iq\mathbf{r}}e^{-i\theta_X}|\uparrow\rangle, \quad (43)$$

where  $n_X = N_X/S$  is the exciton density. We thus see that dissociation of the biexciton condensate produces spontaneous exciton supercurrent

$$\mathbf{j}_X = \frac{\hbar \mathbf{q}}{m_X} n_X. \quad (44)$$

This result is consistent with the broken time-reversal symmetry of the model (21). The exciton supercurrent (44) vanishes almost simultaneously with the residues of the biexciton condensate near the second-order ray  $\{\mu = \varepsilon/2, \mu_B g B > |\varepsilon|/2\}$  (Fig. 1). In the limit  $qa \ll 1$  the solution of the equation  $\partial h_X / \partial q = 0$  takes a simple form

$$q = \frac{m_X v}{\hbar} (\sqrt{4\pi n_B a^2} - \frac{1}{2}), \quad (45)$$

which yields

$$\mu_0 = \left( \frac{1}{2} + \frac{1}{32\pi} \right) \bar{g}^{-1} \varepsilon$$

for the chemical potential at which the state (43) becomes an ordinary  $\sigma^+$ -polarized exciton condensate.

Following the logic of our historical discussion, we dub this state *biexciton Mott supercurrent*. This high-density phase between the biexciton and the exciton BEC's may be compared with the BCS side of the ordinary  $s$ -wave biexciton Mott transition [67]. On the contrary, there is a qualitative difference from the BCS-BEC transition in the narrow-resonance  $s$ -wave FA model, where the biexciton BEC is stabilized at high densities [53].

In TMD monolayers, the domain of existence of this state in the phase diagram shown in Fig. 1 seems to be reduced to a narrow window around the critical end point  $(b_c, \mu_c) = (\frac{1}{2}|\varepsilon|, -\frac{1}{2}|\varepsilon|)$ . For instance, the version on the left has been obtained for  $E_a^{(X)}/|\varepsilon| = 0.8$ , which we believe to be an upper bound for the strength of SO coupling in a typical monolayer of MoS<sub>2</sub>. The point on the second-order line used to illustrate the closure of the roton gap corresponds to  $n_B a^2 = 0.2$ . At such densities the underlying fermionic structure of excitons and biexcitons comes into play, and the actual dissociation scenario may be very different from our predictions [71].

One could try to reduce the biexciton binding energy  $|\varepsilon|$  by working with dipolar excitons in (homo)bilayers. Spatial separation of electrons and holes would also enable experimental detection of the supercurrent following the proposal of Ref. [72], referred to as ‘‘counterflow superconductivity.’’ Another appealing property of the dipolar excitons is their relatively long lifetime  $\tau_X$ . However, the SO coupling (which scales as  $\tau_X^{-1}$  [20]) would be suppressed and the eventual behavior of the ratio  $E_a^{(X)}/|\varepsilon|$  is not evident. A more elaborated study is needed to explore this possibility.

In this regard, we point out affinity of the biexciton Mott supercurrent to the spontaneously polarized exciton superstripe predicted in Ref. [27]. Enhancement of the molecular SO field (40) in that case occurs due to the divergent growth of the biexciton size  $a$  on approaching the critical distance between the layers at which a true bound state turns into a natural resonance [53,54]. The divergence of  $a$  compensates the vanishing strength of the SO coupling and enables the corresponding transition already in the dilute limit. Despite the important differences in their properties, the two phases

are common in that both are manifestations of the  $d$ -wave SO dressing at the many-body level.

## V. CONCLUDING REMARKS

Finally, we point out possible existence of analogous mechanisms for fermions. Replacement of the commutation relations results, in particular, in a sign change in Eq. (22). Consistently, the time-reversal invariance now dictates that  $\Omega(\mathbf{k}) = -\Omega(-\mathbf{k})$ , which is the case for the Rashba [73,74] and Dresselhaus [75] SO couplings. The second-quantized forms of the type (21) then imply intriguing mean-field possibilities associated with topological properties of the Bogoliubov transformation and the existence of chiral edge modes [76,77]. Such possibilities have indeed been anticipated for SO coupled superconductors [78–80] and ultracold fermionic atoms [81], though from a somewhat different perspective. Optical studies of the effects predicted in this work would help to elucidate common fundamental origin of the synthetic orbital momenta of quasiparticles (fermions or bosons) under SO coupling.

## ACKNOWLEDGMENTS

I am grateful to A. V. Kavokin and other colleagues for a helpful reading of the manuscript. I also thank M. I. Dyakonov for an enlightening discussion on the history of electronic SO coupling in crystals. The work could have been supported by Russian Science Foundation (Grant No 22-72-10032). I am indebted to my dear friends Alexandra and Eugene Kogan for their hospitality during my stay in the Moscow region.

## APPENDIX A: PAIR BUBBLES FOR EXCITONS AND POLARITONS

The Gaussian *Ansatz* for the  $s$ -wave biexciton wave function yields the following expressions (we use the units  $E_a^{(\alpha)}$ ):

$$\Pi_X(E + i0) = \pi E^3 G_{4,5}^{3,2}(E^2 |_{-3/2, -1, 0, -7/4, -5/4}^{-3/2, -1, -7/4, -5/4}) - i\pi E^3 \quad (A1)$$

and

$$\begin{aligned} \Pi_L(E + i0) \\ = -\eta^2(1 + E - e^{-E} E^2 [\text{Chi}(E) + \text{Shi}(E)]) + i\pi e^{-E} E^2 \end{aligned} \quad (A2)$$

for the exciton and polariton pair bubbles, respectively. Here  $G_{p,q}^{m,n}(z |_{b_1, \dots, b_m, b_{m+1}, \dots, b_q}^{a_1, \dots, a_n, a_{n+1}, \dots, a_p})$  is the Meijer  $G$  function,  $\text{Chi}(x)$  and  $\text{Shi}(x)$  are the hyperbolic cosine and sine integrals, respectively. As it should be, the real parts of the pair bubbles vanish at  $E \rightarrow \infty$ , whereas their low-energy expansion yields the results presented in the main text.

We note that the coefficient at the first power of  $E$  in the expansion of  $\Pi_\alpha(E + i0)$  defines the relative weight of the halo in the wave function of the synthetic molecule. Interestingly, this coefficient turns out to be the same for few other physical *Ansätze* such as the Coulomb

$$\tilde{\phi}(\mathbf{k}) = \sqrt{\frac{2}{\pi}} \frac{a}{(1 + k^2 a^2)^{3/2}} \quad (A3)$$

and the weakly bound state

$$\tilde{\phi}(\mathbf{k}) = \frac{a}{\sqrt{\pi}} \frac{1}{1 + (ka)^2}, \quad (\text{A4})$$

although the use of the latter would require more elaborated consideration of our model.

Somewhat different but more transparent results may be obtained by using the Heaviside theta function *Ansatz*  $\tilde{\phi}(\mathbf{k}) = a\theta(a^{-1} - k)$ :

$$\begin{aligned} \Pi_X(E + i0) &= -\frac{\pi}{2} \left[ \frac{1}{3} + \frac{E}{2} + E^2 + E^3 \ln\left(\frac{1-E}{E}\right) + i\pi E^3 \right] \end{aligned} \quad (\text{A5})$$

and

$$\Pi_L(E + i0) = -\eta^2 \pi \left[ \frac{1}{2} + E + E^2 \ln\left(\frac{1-E}{E}\right) + i\pi E^2 \right] \quad (\text{A6})$$

for excitons and polaritons, respectively. The Heaviside *Ansatz*, however, has a nonphysical algebraic decay in real space.

## APPENDIX B: DISTORTION OF THE CONTINUUM BY THE BACKGROUND REPULSIVE POTENTIAL

Here we estimate corrections to the pair bubbles due to the distortion of the continuum states by the background repulsive potential  $V_{\uparrow\uparrow}^{(\alpha)}(r)$ . We start with the general expression for the pair bubble

$$\Pi_\alpha(E + i0) = \hbar^2 \int \frac{\langle \varphi | \hat{\Omega}_\alpha | \mathbf{q} \rangle \langle +\mathbf{q} | \hat{\Omega}_\alpha^\dagger | \varphi \rangle}{E - E_q^{(L)} + i0} d\mathbf{q}, \quad (\text{B1})$$

where we have introduced the operator

$$\hat{\Omega}_\alpha = \int \sqrt{2} \Omega_\alpha^{(s)}(\mathbf{k}) \cdot s_{\uparrow\downarrow} |\mathbf{k}\rangle \langle \mathbf{k}| d\mathbf{k} \quad (\text{B2})$$

and  $|\mathbf{q}\rangle$  are the background scattering states. For definitiveness, let us consider polaritons. The scattering states can be recast as

$$|\mathbf{q}\rangle = |\mathbf{q}\rangle + G_{0,\uparrow\uparrow}^{(L)}(E_q^{(L)} + i0) T_{\uparrow\uparrow,\text{bg}}^{(L)}(E_q^{(L)} + i0) |\mathbf{q}\rangle, \quad (\text{B3})$$

where  $G_{0,\uparrow\uparrow}^{(L)}(z)$  and  $T_{\uparrow\uparrow,\text{bg}}^{(L)}(z)$  are the free Green operator and the background  $T$  operator of the polariton open channel. Furthermore, we write

$$\begin{aligned} &\langle \varphi | \hat{\Omega}_L | \mathbf{q} \rangle \\ &= \int \frac{\sqrt{2} \Omega_L(\mathbf{k}) \cdot s_{\uparrow\downarrow} \langle \varphi | \mathbf{k} \rangle \langle \mathbf{k} | T_{\uparrow\uparrow,\text{bg}}^{(L)}(E_q^{(L)} + i0) | \mathbf{q} \rangle}{E_q^{(L)} - E_k^{(L)} + i0} d\mathbf{k}. \end{aligned} \quad (\text{B4})$$

Let us model  $V_{\uparrow\uparrow}^{(L)}(r)$  by the impenetrable-disk potential of the radius  $a$ . The off-shell  $T$  matrix then can be expressed as [82]

$$\begin{aligned} &\langle \mathbf{k} | T_{\uparrow\uparrow,\text{bg}}^{(L)}(E_q^{(L)} + i0) | \mathbf{q} \rangle \\ &= (2\pi)^{-2} \frac{\hbar^2}{m} q a \sum_{m=0}^{+\infty} c_m e^{i\delta_m(q)} J_m(ka) \\ &\quad \times [\cos(\delta_m) J_{m+1}(qa) - \sin(\delta_m) Y_{m+1}(qa)] \cos(m\theta), \end{aligned} \quad (\text{B5})$$

where  $c_m = 1$  for  $m = 0$  and  $c_m = 2$  otherwise, and the sine and cosine of the scattering phase shift are given by

$$\cos(\delta_m) = \frac{Y_m(qa)}{\sqrt{J_m^2(qa) + Y_m^2(qa)}}, \quad (\text{B6a})$$

$$\sin(\delta_m) = \frac{J_m(qa)}{\sqrt{J_m^2(qa) + Y_m^2(qa)}}. \quad (\text{B6b})$$

Due to the orbital dependence of the matrix element

$$\hbar \Omega_L(\mathbf{k}) \cdot s_{\uparrow\downarrow} = -\frac{\hbar^2 k^2}{m_{\text{LT}}} e^{-2i\theta}, \quad (\text{B7})$$

only the  $d$  waves from the background scattering contribute to the pair-bubble equation (B1). By taking the Heaviside theta *Ansatz*  $\langle \mathbf{k} | \varphi \rangle = a\theta(a^{-1} - k)$  and performing the integration, one obtains the leading correction to the unperturbed result [the above Eq. (A6)]

$$\frac{\delta \Pi_L}{E_a^{(L)}} = -2^{-15} \pi^{-1} \eta^2. \quad (\text{B8})$$

We therefore conclude that the background distortion of the continuum may be safely neglected.

- 
- [1] P. G. Kwiat, K. Mattle, H. Weinfurter, A. Zeilinger, A. V. Sergienko, and Y. Shih, *Phys. Rev. Lett.* **75**, 4337 (1995).
- [2] A. N. Boto, P. Kok, D. S. Abrams, S. L. Braunstein, C. P. Williams, and J. P. Dowling, *Phys. Rev. Lett.* **85**, 2733 (2000).
- [3] A. Lamas-Linares, J. C. Howell, and D. Bouwmeester, *Nature (London)* **412**, 887 (2001).
- [4] S. L. Braunstein and P. van Loock, *Rev. Mod. Phys.* **77**, 513 (2005).
- [5] C. L. Salter, R. M. Stevenson, I. Farrer, C. A. Nicoll, D. A. Ritchie, and A. J. Shields, *Nature (London)* **465**, 594 (2010).
- [6] A. Dousse, J. Suffczyński, A. Beveratos, O. Krebs, A. Lemaître, I. Sagnes, J. Bloch, P. Voisin, and P. Senellart, *Nature (London)* **466**, 217 (2010).
- [7] P. Tamarat, L. Hou, J.-B. Trebbia, A. Swarnkar, L. Biadala, Y. Louyer, M. I. Bodnarchuk, M. V. Kovalenko, J. Even, and B. Lounis, *Nat. Commun.* **11**, 6001 (2020).
- [8] J. Q. Grim, S. Christodoulou, F. Di Stasio, R. Krahné, R. Cingolani, L. Manna, and I. Moreels, *Nat. Nanotechnol.* **9**, 891 (2014).
- [9] R. C. Miller, D. A. Kleinman, A. C. Gossard, and O. Munteanu, *Phys. Rev. B* **25**, 6545 (1982).
- [10] T. Kondo, T. Azuma, T. Yuasa, and R. Ito, *Solid State Commun.* **105**, 253 (1998).
- [11] E. J. Sie, A. J. Frenzel, Y.-H. Lee, J. Kong, and N. Gedik, *Phys. Rev. B* **92**, 125417 (2015).
- [12] Y. You, X.-X. Zhang, T. C. Berkelbach, M. S. Hybertsen, D. R. Reichman, and T. F. Heinz, *Nat. Phys.* **11**, 477 (2015).



- [13] K. Hao, J. F. Specht, P. Nagler, L. Xu, K. Tran, A. Singh, C. K. Dass, C. Schüller, T. Korn, M. Richter, A. Knorr, X. Li, and G. Moody, *Nat. Commun.* **8**, 15552 (2017).
- [14] Z. Li, T. Wang, Z. Lu, C. Jin, Y. Chen, Y. Meng, Z. Lian, T. Taniguchi, K. Watanabe, S. Zhang, D. Smirnov, and S.-F. Shi, *Nat. Commun.* **9**, 3719 (2018).
- [15] F. Thouin, S. Neutzner, D. Cortecchia, V. A. Dragomir, C. Soci, T. Salim, Y. M. Lam, R. Leonelli, A. Petrozza, Ajay Ram Srimath Kandada, and C. Silva, *Phys. Rev. Mater.* **2**, 034001 (2018).
- [16] S. V. Andreev, *Phys. Rev. B* **101**, 125129 (2020).
- [17] G. E. Pikus and G. L. Bir, *Zh. Eksp. Teor. Fiz.* **60**, 195 (1971) [*Sov. Phys. JETP* **33**, 195 (1970)].
- [18] M. Z. Maialle, E. A. de Andrada e Silva, and L. J. Sham, *Phys. Rev. B* **47**, 15776 (1993).
- [19] S. V. Gupalov, E. L. Ivchenko, and A. V. Kavokin, *J. Exp. Theor. Phys.* **86**, 388 (1998).
- [20] M. M. Glazov, T. Amand, X. Marie, D. Lagarde, L. Bouet, and B. Urbaszek, *Phys. Rev. B* **89**, 201302(R) (2014).
- [21] D. Y. Qiu, T. Cao, and S. G. Louie, *Phys. Rev. Lett.* **115**, 176801 (2015).
- [22] H. Yu, X. Cui, X. Xu, and W. Yao, *Natl. Sci. Rev.* **2**, 57 (2015).
- [23] M. O. Nestoklon, S. V. Goupalov, R. I. Dzhiyev, O. S. Ken, V. L. Korenev, Y. G. Kusrayev, V. F. Sapega, C. de Weerd, L. Gomez, T. Gregorkiewicz, J. Lin, K. Suenaga, Y. Fujiwara, L. B. Matyushkin, and I. N. Yassievich, *Phys. Rev. B* **97**, 235304 (2018).
- [24] G. Panzarini, L. C. Andreani, A. Armitage, D. Baxter, M. S. Skolnick, V. N. Astratov, J. S. Roberts, A. V. Kavokin, M. R. Vladimirova, and M. A. Kaliteevski, *Phys. Rev. B* **59**, 5082 (1999).
- [25] A. Kavokin, G. Malpuech, and M. Glazov, *Phys. Rev. Lett.* **95**, 136601 (2005).
- [26] O. Bleu, D. D. Solnyshkov, and G. Malpuech, *Phys. Rev. B* **96**, 165432 (2017).
- [27] S. V. Andreev, *Phys. Rev. B* **103**, 184503 (2021).
- [28] A. J. Moerdijk, B. J. Verhaar, and A. Axelsson, *Phys. Rev. A* **51**, 4852 (1995).
- [29] A. S. Jensen, K. Riisager, D. V. Fedorov, and E. Garrido, *Rev. Mod. Phys.* **76**, 215 (2004).
- [30] E. Hanamura, *Phys. Rev. B* **38**, 1228 (1988).
- [31] C. Weisbuch, M. Nishioka, A. Ishikawa, and Y. Arakawa, *Phys. Rev. Lett.* **69**, 3314 (1992).
- [32] F. ěulik, *Czech J. Phys.* **16**, 194 (1966).
- [33] J. J. Forney, A. Quattropani, and F. Bassani, *Nuovo Cimento B* **22**, 153 (1974).
- [34] A. I. Bobrysheva, V. T. Zyukov, and S. I. Beryl, *Phys. Status Solidi B* **101**, 69 (1980).
- [35] D. Xiao, G.-B. Liu, W. Feng, X. Xu, and W. Yao, *Phys. Rev. Lett.* **108**, 196802 (2012).
- [36] M. R. Molas, A. O. Slobodeniuk, T. Kazimierzczuk, K. Nogajewski, M. Bartos, P. Kapuściński, K. Oreszczuk, K. Watanabe, T. Taniguchi, C. Faugeras, P. Kossacki, D. M. Basko, and M. Potemski, *Phys. Rev. Lett.* **123**, 096803 (2019).
- [37] M. I. Sheboul and W. Ekardt, *Phys. Status Solidi B* **73**, 165 (1976).
- [38] B. Piętko, D. Zygunt, M. Król, M. R. Molas, A. A. L. Nicolet, F. Morier-Genoud, J. Szczytko, J. Łusakowski, P. Zieba, I. Tralle, P. Stepnicki, M. Matuszewski, M. Potemski, and B. Deveaud, *Phys. Rev. B* **91**, 075309 (2015).
- [39] A. V. Stier, N. P. Wilson, K. A. Velizhanin, J. Kono, X. Xu, and S. A. Crooker, *Phys. Rev. Lett.* **120**, 057405 (2018).
- [40] A. I. Akhiezer and V. B. Berestetskii, *Quantum Electrodynamics* (Interscience, New York, 1965).
- [41] In TMD's the absence of an inversion center implies that the spin states  $|\uparrow\rangle$  and  $|\downarrow\rangle$  are additionally locked to the  $\mathbf{K}_+$  and  $\mathbf{K}_-$  valleys, respectively.
- [42] Consider  $s_x = \psi_\uparrow^* \psi_\downarrow + \psi_\downarrow^* \psi_\uparrow$  and  $s_z = |\psi_\uparrow|^2 - |\psi_\downarrow|^2$ . Under time reversal the components of a spinor transform as  $\psi_{s,\sigma} \rightarrow \psi_{s,-\sigma}^* (-1)^{s+\sigma}$ . In our case  $s = 1$  and  $\sigma = +1, -1$ . One obtains  $\psi_\uparrow \rightarrow \psi_\downarrow^*$  and  $\psi_\downarrow \rightarrow \psi_\uparrow^*$ . One has  $s_x \rightarrow s_x$  and  $s_z \rightarrow -s_z$ , as one would indeed expect for the linear and circular polarization degrees, respectively.
- [43] G. Sallen, L. Bouet, X. Marie, G. Wang, C. R. Zhu, W. P. Han, Y. Lu, P. H. Tan, T. Amand, B. L. Liu, and B. Urbaszek, *Phys. Rev. B* **86**, 081301(R) (2012).
- [44] H. Zeng, J. Dai, W. Yao, D. Xiao, and X. Cui, *Nat. Nanotechnol.* **7**, 490 (2012).
- [45] A. Srivastava, M. Sidler, A. V. Allain, D. S. Lembke, A. Kis, and A. Imamoglu, *Nat. Phys.* **11**, 141 (2015).
- [46] H. H. Fang, B. Han, C. Robert, M. A. Semina, D. Lagarde, E. Courtade, T. Taniguchi, K. Watanabe, T. Amand, B. Urbaszek, M. M. Glazov, and X. Marie, *Phys. Rev. Lett.* **123**, 067401 (2019).
- [47] N. S. Voronova, I. L. Kurbakov, and Y. E. Lozovik, *Phys. Rev. Lett.* **121**, 235702 (2018).
- [48] D. B. Cassidy, *Eur. Phys. J. D* **72**, 53 (2018).
- [49] *Collected Papers of L.D. Landau*, edited by D. Ter Haar (Pergamon, Oxford, 1965), pp. 471–473.
- [50] C. N. Yang, *Phys. Rev.* **77**, 242 (1950).
- [51] A. Ivanov, H. Haug, and L. Keldysh, *Phys. Rep.* **296**, 237 (1998).
- [52] A. J. C. Varandas, J. da Providência, M. Brajczewska, and J. P. da Providência, *Eur. Phys. J. D* **69**, 114 (2015).
- [53] S. V. Andreev, *Phys. Rev. B* **92**, 041117(R) (2015).
- [54] S. V. Andreev, *Phys. Rev. B* **94**, 140501(R) (2016).
- [55] A. Maruani and D. S. Chemla, *Phys. Rev. B* **23**, 841 (1981).
- [56] J. R. Taylor, *Scattering Theory* (Dover, Mineola, New York, 2006).
- [57] U. Fano, *Phys. Rev.* **124**, 1866 (1961).
- [58] P. W. Anderson, *Phys. Rev.* **124**, 41 (1961).
- [59] E. Timmermans, P. Tommasini, M. Hussein, and A. Kerman, *Phys. Rep.* **315**, 199 (1999).
- [60] L. Radzihovsky, J. Park, and P. B. Weichman, *Phys. Rev. Lett.* **92**, 160402 (2004).
- [61] V. Gurarie and L. Radzihovsky, *Ann. Phys.* **322**, 2 (2007), January Special Issue 2007.
- [62] A. Mair, A. Vaziri, G. Weihs, and A. Zeilinger, *Nature (London)* **412**, 313 (2001).
- [63] J. G. Valatin and D. Butler, *Nuovo Cimento* **10**, 37 (1958).
- [64] M. Girardeau and R. Arnowitt, *Phys. Rev.* **113**, 755 (1959).
- [65] A. Coniglio and M. Marinaro, *Nuovo Cimento B* **48**, 249 (1967).
- [66] W. A. B. Evans and Y. Imry, *Nuovo Cimento B* **63**, 155 (1969).
- [67] P. Nozières and D. Saint James, *J. Phys. (France)* **43**, 1133 (1982).
- [68] K. Mavroyannis, *Phys. Rev. B* **10**, 1741 (1974).
- [69] V. M. Nandakumaran and K. P. Sinha, *Z Phys. B* **22**, 173 (1975).
- [70] A. I. Bobrysheva, S. A. Moskalenko, and Y. M. Shvera, *Phys. Status Solidi B* **147**, 711 (1988).

- [71] G. Röpke, A. Schnell, P. Schuck, and P. Nozières, *Phys. Rev. Lett.* **80**, 3177 (1998).
- [72] Y. E. Lozovik and V. I. Yudson, *Pis'ma Zh. Eksp. Teor. Fiz.* **22**, 556 (1975) [*Sov. Phys. JETP* **44**, 389 (1976)].
- [73] F. T. Vas'ko, *Pis'ma Zh. Eksp. Teor. Fiz.* **30**, 574 (1979) [*Sov. Phys. JETP Lett.* **30**, 541 (1979)].
- [74] Y. A. Bychkov and E. I. Rashba, *Pis'ma Zh. Eksp. Teor. Fiz.* **39**, 66 (1984) [*Sov. Phys. JETP Lett.* **39**, 78 (1984)].
- [75] M. I. Dyakonov and Yu. V. Kachorovskii, *Fiz. Techn. Poluprov.* **20**, 178 (1986) [*Sov. Phys. Semicond.* **20**, 110 (1986)].
- [76] N. Read and D. Green, *Phys. Rev. B* **61**, 10267 (2000).
- [77] S. V. Andreev (unpublished).
- [78] L. Fu and C. L. Kane, *Phys. Rev. Lett.* **100**, 096407 (2008).
- [79] J. D. Sau, R. M. Lutchyn, S. Tewari, and S. Das Sarma, *Phys. Rev. Lett.* **104**, 040502 (2010).
- [80] J. Alicea, *Phys. Rev. B* **81**, 125318 (2010).
- [81] C. Zhang, S. Tewari, R. M. Lutchyn, and S. Das Sarma, *Phys. Rev. Lett.* **101**, 160401 (2008).
- [82] M. Schick, *Phys. Rev. A* **3**, 1067 (1971).